

Weathering rind characteristics of blocky deposits in a deglaciated cirque on Mt. Yakushi, the Northern Japanese Alps

Chiaki T. Oguchi, Takeshi Noda* and Norikazu Matsuoka

Introduction

Weathering-rind thickness (WRT) has been used as an indicator of relative ages of glacial and periglacial deposits in high mountain areas (*e.g.* Birkeland, 1973; Koizumi and Aoyagi, 1993; Aoki, 2000). The method is simple and useful but may include errors arising from the difference in weathering environments or personal identification of the rind. This paper discusses the relationship between the visual determination of WRT and chemical weathering processes, based on the field measurement and chemical analysis of rinds developed on blocky deposits in a deglaciated cirque.

The study area

The study area is located on Mt. Yakushi (2926 m ASL), the Northern Japanese Alps. The summit area shows an asymmetrical ridge with periglacial smooth slopes on the west-facing side and cirques on the east-facing side (*e.g.* Takada, 1992). A large amount of snowfall and strong northwesterly wind provide deep snow in these cirques during winter. Most of the snow remains until late summer and some snow patches are perennial. The field survey was undertaken in the Kinsaku-dani cirque (Figs. 1-2), which virtually consists of a single lithology, quartz-porphry. This lithology merits the analysis, because of the rind development with a distinct visual front (Koizumi and Aoyagi, 1993).

The Kinsaku-dani cirque is 650 m wide and 200 m deep. The cirque floor has four series of blocky ridges (A-D: Figs. 1-2).

Ridge A consists of two short ridges 5 m wide and 2 m high, lying only at the foot of the north-facing rockwall. Koizumi and Aoyagi (1993) have regarded the ridge as a protalus rampart produced by supra-nival debris transport, but another possibility is that this is an inner pressure ridge of a rock glacier. The ridge is composed mainly of large boulders with a diameter of *ca.* 1 m lacking interstitial fine materials.

Ridge B is the longest, continuous ridge 10 m wide and 5 m high at the largest part, displaying a M-shape in plan (Fig. 2). This ridge has long been considered to be the terminal moraine of the latest glaciation (*e.g.*

Koizumi and Aoyagi, 1993), but this interpretation is problematic. Firstly, the distance between the ridge and rockwall is too short for a small glacier to produce such a distinct moraine ridge (in particular, at the northern part; see Fig. 2). Secondly, outwash streams usually collapse part of the terminal moraine of mountain glaciers, but the M-shaped ridge lacks such dissection. Another explanation for Ridge B is the outermost ridge of a rock glacier depressed by partial or complete ice melting (Matsuoka and Ikeda, 1998; see also Barsch, 1996). Boulders with a diameter of *ca.* 30 cm are dominant on the ridge. The ridge is partially vegetated with *Pinus Pumila*.

Ridge C, 5 m wide and 2 m high, lies only in the southern part of the cirque (Fig. 1). In northern part this ridge converges to Ridge B. The ridge is composed mainly of angular gravel with a diameter of 10-30 cm filled with nonsorted sandy matrix. Half of the ridge is vegetated. This ridge may be part of a terminal moraine. On this assumption, after the deglaciation a talus-derived lobate rock glacier (Ridge B) would have grown and overridden the moraine.

Ridge D is not a continuous ridge but composed of small mounds (Fig. 2). Sub-rounded boulders with a diameter of 30-100 cm filled with nonsorted sandy soil are dominant on the ridge. A large part of the ridge is vegetated. The ridge was possibly produced as a ground moraine. The associated terminal moraine is absent because the glacier terminus may have fallen into the steep rockwall beyond the edge of the cirque floor; otherwise, a rock avalanche collapsed the terminal moraine after deglaciation.

Field measurement

Weathering rinds are altered coloured zones constituting the outermost part of rocks, which originate from oxidation and dissolution. The rinds grow from the rock surface inward by chemical weathering that begins immediately after the rock is exposed subaerially. Thus, WRT indicates the relative exposure age.

Weathering rinds are observed on gravel composing all ridges on the cirque floor. We measured quartz-porphry boulders with a diameter of more than 20 cm, which are neither buried nor budged. Furthermore, to minimize the difference in weathering environments, measurements

* Forestry Department, Yamanashi Prefectural Government

were undertaken only on the ridges exposed above the snow surface in July. The measurement sites consist of two on Ridge A (A1-A2), sixteen on Ridge B (B1-B16), three on Ridge C (C1-C3) and five on Ridge D (D1-D5). Twenty-five boulders for each site were split with a hammer. The thickness of the brown-coloured rind was determined perpendicular to the upper surface of the boulders. The corners and cracks were avoided from measurement.

Figure 3 summarizes the results. Boulders at Sites A1-A2 have rinds with the mean thickness of 1.2 mm and show histograms with a sharp peak around 1 mm. Boulders on Ridge B show two patterns: the histograms for Sites B1, B2, B7, B11, B13, B14 and B15 display a broad peak of 1-3 mm in thickness, while others have a sharp peak around 1 mm like at Sites A1 and A2. Boulders on Ridge C have rinds with the mean thickness of 4.2 mm, and the histograms show a broad peak around 3-5 mm. Boulders on Ridge D show the mean rind thickness of 6.4 mm. Apart from D4 having a larger peak around 5-10 mm, the histograms for Ridge D display a wide peak around 3-7 mm.

These results demonstrate a significant difference in WRT between the four ridges, suggesting the different production ages of these boulders. An exception is the similar peaks between Sites A1-A2 and B3-B7, which may indicate that these two ridges composed a rock glacier. In addition, the smallest WRT at these sites suggests that the latest activity occurred in this part of the rock glacier.

Rock samples for analysis

Quartz-porphyry blocks are very hard and dense in the interior and have brown weathering rinds (Figs. 4a-b). Two blocks were selected for chemical analyses. One was taken from Site B9 with a weathering rind of 1.8 mm thickness and the other was from Site C3 with a rind of 5.8 mm. The samples were cut into small specimens (Figs. 4c-d), which extend from fresh interior to yellowish-brown rinds.

Visual observation reveals many phenocrysts scattered in a green groundmass. The phenocrysts are white, dark brown and black with the maximum sizes are 3, 2 and 1 mm, respectively. The hardness of the rinds is less than that of the interior, although the rinds cannot be shattered by fingernails. No coatings develop on the surface of the weathering rinds and the yellowish-brown colour extends throughout the rinds. The chromaticness of the colour decreases slightly with depth from the rock surface.

Electron probe microanalysis

Electron probe microanalysis (EPMA) was conducted

to examine the element concentration of the area through the interior to the weathering rind (qualitative mapping) and the chemical composition for micro spots for each zone. Analyses were carried out on a JOEL JXA-8621; the electron probe was operated at 20 kV and the electron beam was focused to 10 μm in diameter.

Figures 5 and 6 show the coloured concentration maps of six elements of the samples from Site B9 and Site C3, respectively. The left edge corresponds to the rock surface. The colour steps of the figures indicate the relative content of each element: white, red, yellow, green, blue and black show decreasing quantity in this order.

The sample from Site B9 (Fig. 5) has no changes in the contents of Si, Fe and K in the groundmass from rock surface to the interior. The contents of Al, Na and Ca in the groundmass decrease gradually outward from the interior to the rind. In particular, the Ca content becomes extremely low in the edge of the rind. The decreasing fronts of Al, Na and Ca are located at *ca.* 1.8 mm depth from the rock surface, which corresponds to visual rind determination. The phenocryst minerals numbered I, which occur only in Si, are quartz. The minerals II and III are K-feldspar and plagioclase, respectively, because the former contains Si, Al and K, and the latter contains Si, Al, Na and Ca. The minerals IV, which occur only in Fe, are magnetite-like minerals.

The contents of Si and Fe in the groundmass of the C3 sample (Fig. 6) decrease in the outermost rind more than in the interior. The content of K in the groundmass slightly decreases in the rind. The contents of Al, Na and Ca in the groundmass decrease gradually outward from the interior to the rind and especially Ca and Na are completely leached out in the outer part of the rind. The decreasing fronts of Al, Na and Ca are located at 5.6-5.8 mm depth from the rock surface, which corresponds to visual rind determination. The phenocryst minerals numbered I-IV are the same as those of the B9 sample. However, the rind of the C3 sample shows some more severely weathered characteristics compared to the B9 sample. Cracks are formed in a large quartz mineral I near the border of the rind and the interior, where the content of Fe is high. The plagioclase III with the arrow in the rind indicates that Si, Ca and Na are dissolved to leave only the framework of the mineral.

Discussion

Field measurement shows that WRT increases in the order of ridges A or B, C and D. Although absolute ages of the ridges are unknown, Ridges A and B may have been formed during the same events and the formation ages of Ridges B, C and D are considered to

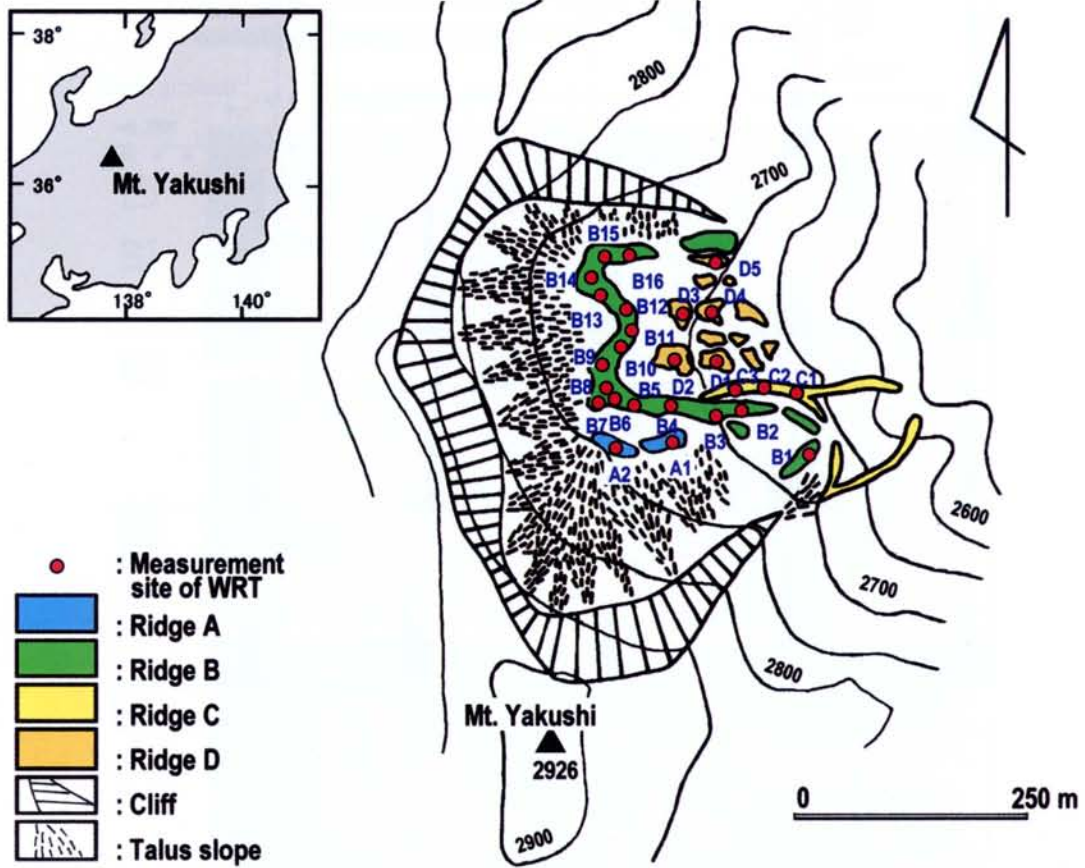


Fig. 1. Geomorphological map of Kinsaku-dani cirque.

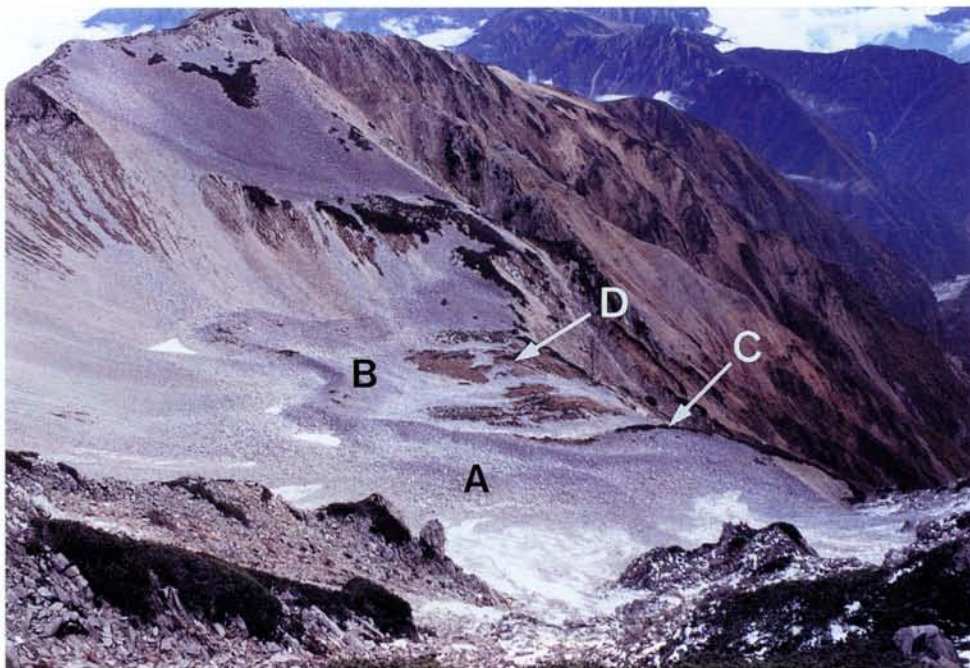


Fig. 2. Ridges A-D in Kinsaku-dani cirque.

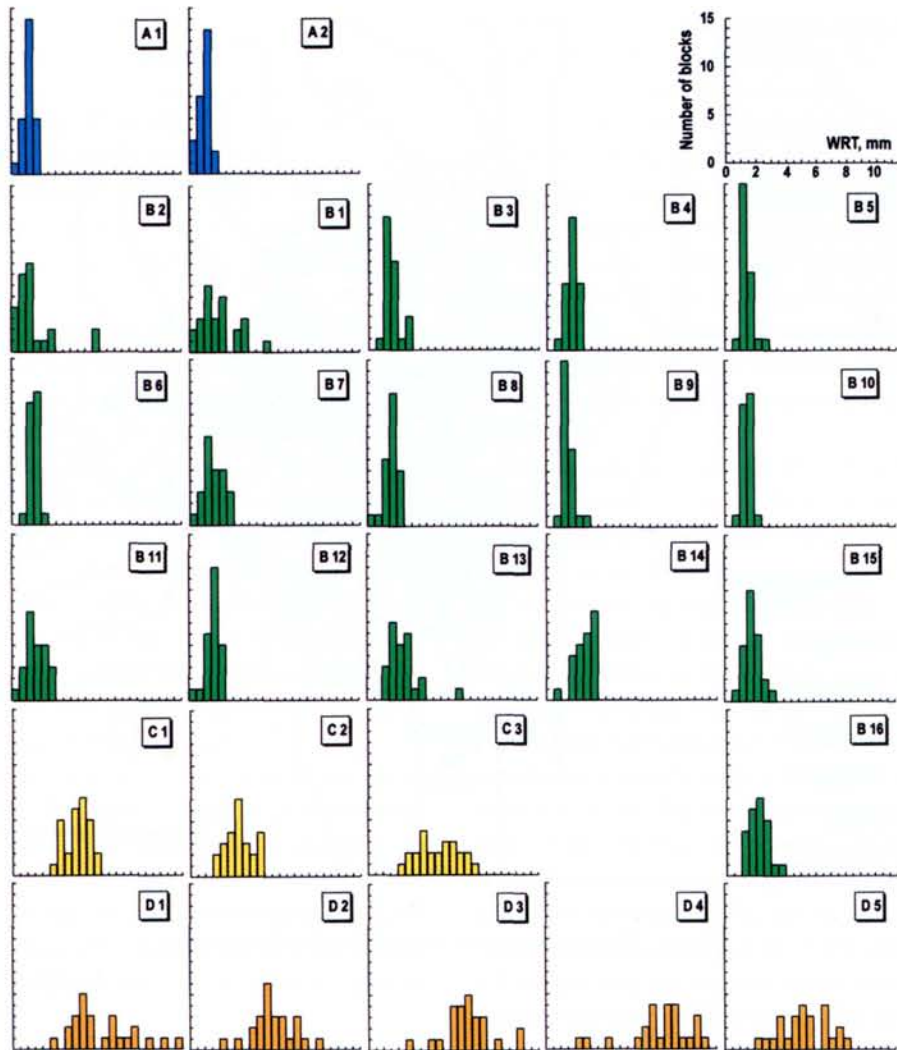


Fig. 3. Results of measurement of weathering-rind thickness (WRT).

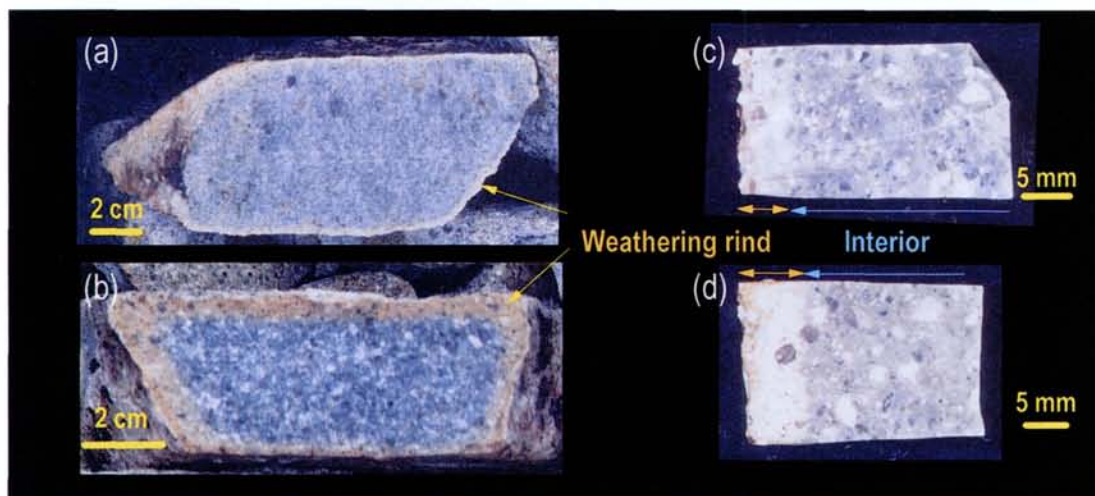


Fig. 4. Quartz-porphry blocks with weathering rinds: blocks of Site B4 (a) and Site D2 (b); specimens for chemical analyses made from B9 block (c) and C3 block (d).

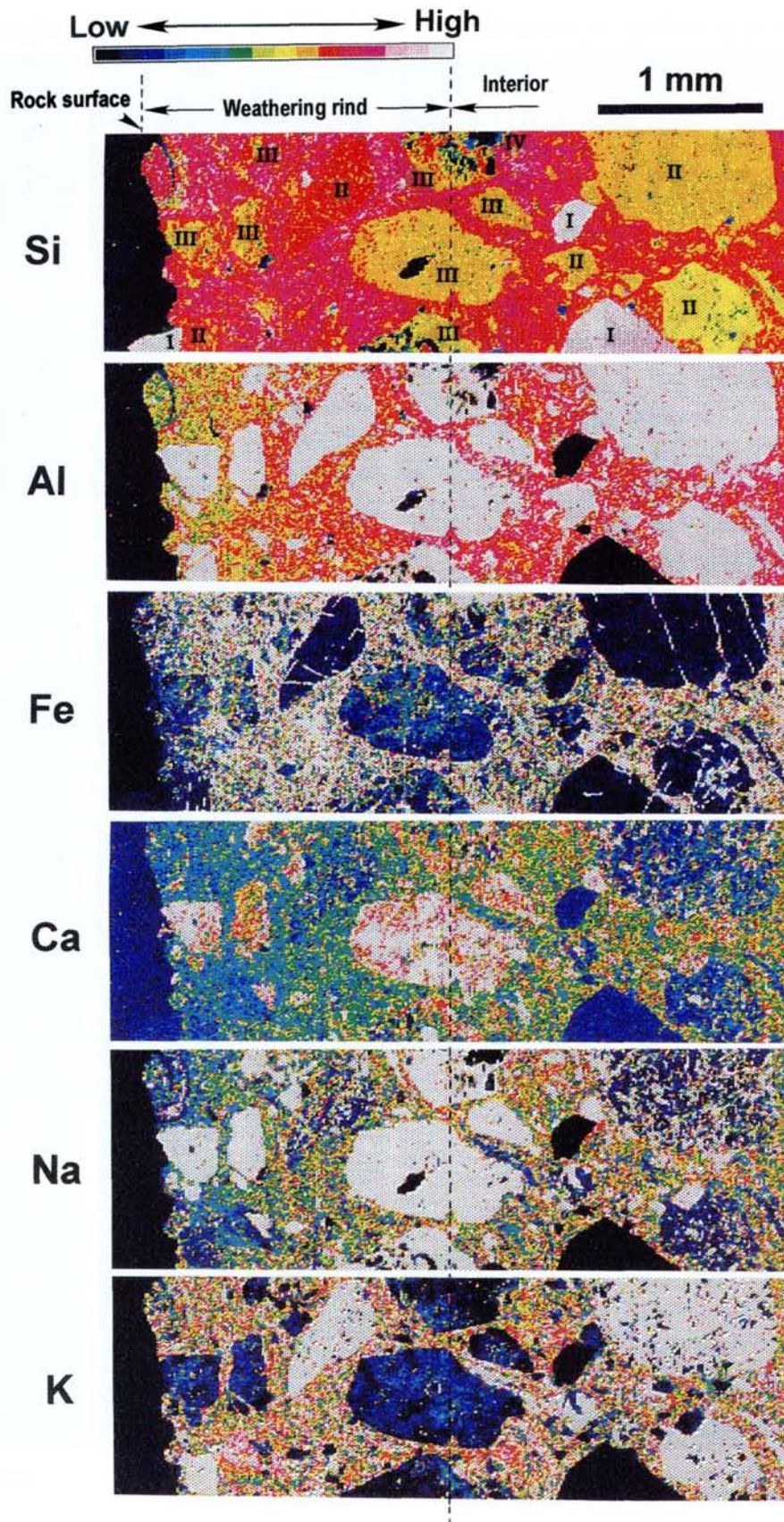


Fig. 5. EPMA element maps of Si, Al, Fe, Ca, Na and K of the sample from Site B9. (I: quartz, II: K-feldspars, III: plagioclase and IV: magnetite-like minerals).

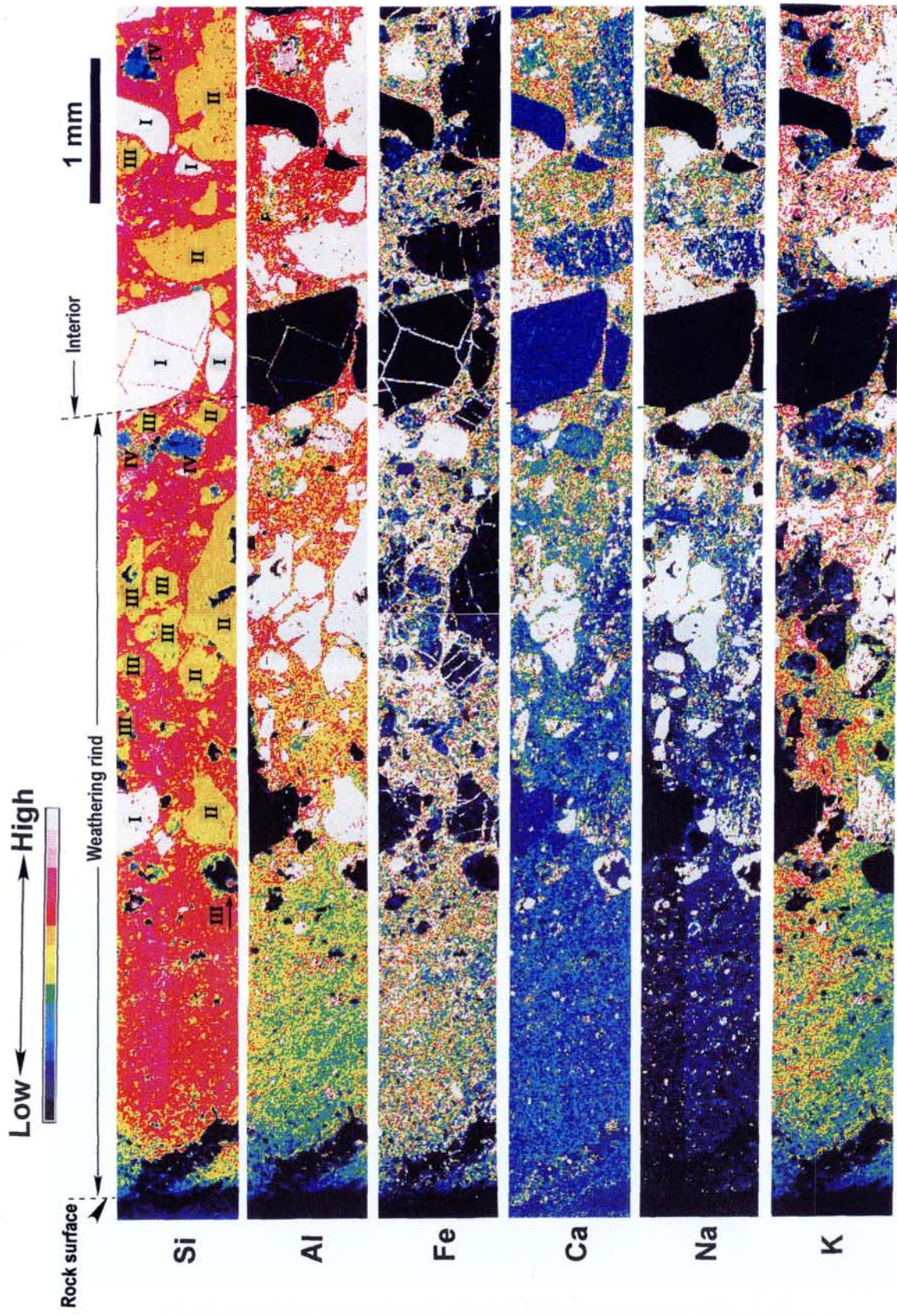


Fig. 6. EPMA element maps of Si, Al, Fe, Ca, Na and K of the sample from Site C3. (I: quartz, II: K-feldspars, III: plagioclase and IV: magnetite-like minerals. The arrows indicate the framework remained plagioclases due to weathering.)

be older in this order.

EPMA mapping data for the B9 and C3 samples show that the original rocks had similar chemical and mineralogical characteristics. Comparing phenocryst minerals of both samples, weathering series of the minerals are considered as follows: groundmass \approx plagioclase < K-feldspar < quartz \approx magnetite-like minerals. Magnetite and quartz are the most stable minerals in the quartz-porphry rocks because the elements in their minerals are not dissolved but cracks occur in the quartz of the weathering rind of the older sample. K-feldspars are the next stable mineral since K of the phenocrysts in the weathering rind is slightly dissolved compared to those in the interior. Plagioclase and groundmass are the weakest components of the rock. Plagioclase in the weathering rind remains only in the framework. Ca and Na in the groundmass are the most dissolved elements compared to the other minerals.

The EPMA data also show that Al, Ca and Na were dissolved from both samples but the other elements did not move significantly. Dissolution of Al and stability of Si in the weathering rinds of both samples indicate that the weathering environment was acidic. This suggests that Fe, originally Fe²⁺ in unweathered rocks, was oxidised to be Fe³⁺ forming the yellowish brown weathering rinds with little changes in the Fe contents. The dissolution front identified from EPMA mapping data approximates the visually determined oxidation front. Furthermore, the rocks are very dense. These results agree with the observation for andesite gravel in the terrace deposits investigated by Oguchi (2001a, b), that the thicknesses of dissolution rinds and oxidation rinds are almost equal if the host rock has a low porosity.

The formation processes of weathering rinds on quartz-porphry rocks are also comparable to those on

andesite gravel in terrace deposits. Dissolution and oxidation are predominant and WRT is easily determinable as a brown rind if the rocks are very dense. In the case of the four ridges made of quartz-porphry blocks in the Kinsaku-dani cirque, visually determined WRT is useful to estimate the relative ages of their formation. However, the application of the WRT measurement to porous rocks needs caution because the coincidence between dissolution rinds and oxidation rinds has not yet been verified. The visual determination of WRT in the field should be accompanied by porosity data for the unweathered rock and colour information of weathering rinds.

Acknowledgements

We are grateful to Dr. Kosei Komuro and Mr. Norimasa Nishida for valuable advice regarding element mapping using EPMA.

References

- Aoki, T. (2000): *Geogr. Rev. Jap.*, **73B**, 105-118.
 Barsch, D. (1996): *Rockglaciers: indicators for the present and former geocology in high mountain environments*. 331 p. Springer, Berlin.
 Birkeland, P. W. (1973): *Arct. Alp. Res.*, **5**, 401-416.
 Koizumi, T. and Aoyagi, S. (1993): *Geogra. Rev. Jap.*, **66A**, 269-286 (in Japanese with English abstract).
 Matsuoka, N. and Ikeda, A. (1998): *Ann. Rep., Inst. Geosci., Univ. Tsukuba*, **24**, 19-25.
 Oguchi, C. T. (2001a): *Earth Surf. Process. Landforms*, **26**, 847-858.
 Oguchi, C. T. (2001b): *Abst. 5th Int. Conf. Geomorph.* (Tokyo), 172.
 Takada, M. (1992): *J. Geogr. (Tokyo)*, **101**, 594-614.

Keywords: weathering rind, relative age, cirque, electron probe microanalysis